SUBMITTED TO:

Mr. James Dobrowolski
USDA/ National Institute of Food and Agriculture

Final Report

A Thermal Distillation Process for Expanding Water Resources

October 31, 2022

Award No. 2019-33610-30171

SUBMITTED BY:

AIL Research, Inc.
57 Hamilton Ave
Hopewell, NJ 08525

A Thermal Distillation Process for Expanding Water Resources

Identification and Significance of the Problem or Opportunity

A large majority of the world's freshwater usage goes to agriculture – estimates put agricultural needs worldwide at around 70% of all human use. Furthermore, agriculture's use of water is still increasing globally due not only to population growth, but also due to higher plant transpiration rates driven by increasing ambient temperatures. In many parts of the world this has led to significant drops in the level of groundwater as it is pumped out faster than it can recharge.

In California, where more than 60% of the U.S. fruits and vegetables are grown, agriculture accounts for approximately 80% of water use. The state estimates that groundwater is being overpumped by at least 2.5 million acre-feet per year leading to twenty-one of the state's groundwater basins being identified as critically over-drafted. Under California's new Sustainable Groundwater Management Act, over 1 million irrigated acres in California, 10% of the state's total, are at risk being forced to be fallowed unless new water supplies are found.

However, in California and elsewhere while freshwater reserves in the ground are shrinking brackish groundwater[1] reserves are growing. This growth in brackish groundwater is mainly due to salts brought in with irrigation water, seawater intrusion in coastal zones or agricultural runoff. For example, it is estimated that in California's Central Valley salts are building up at a rate of 700 million tons per year due to both the importation of irrigation water from the mountains and agricultural runoff high in nitrates.

Brackish groundwater is mostly unusable for agriculture. As groundwater salts increase over 500 TDS, plants grow more slowly, yield less, require more water, and suffer greater mortality. Salt buildup in agricultural basins is increasingly viewed as a long-term threat comparable to water shortage.

Recent surveys have identified tens of billions of acre-feet of brackish groundwater underlying significant portions of the U.S. California alone has hundreds of millions of acre-feet of brackish groundwater—over one-fourth of all the water in the state. The use of these brackish groundwater reserves for agriculture could significantly ease over pumping of neighboring fresh groundwater reserves allowing them to recharge.

So why aren't we desalinating brackish groundwater for agriculture? The simple answer is that costs are much too high. Even for high value crops farmers can only afford to pay around $0.60 per cubic meter[2] for water—a price that is about one-third that for potable water produced by the Carlsbad and Santa Barbara reverse-osmosis seawater desalination plants.

With as little as 1/30th the salt concentration of seawater, brackish water should be less expensive to desalinate. However, a breakdown of the costs to desalinate brackish water shows that the process is heavily penalized by the cost of waste brine disposal. If disposal costs are ignored, a reverse osmosis facility could convert as much as 90% of brackish water to freshwater at a cost of $0.40 per cubic meter. However, the 10% stream of waste brine with high salt concentrations presents an almost impossible disposal challenge, costing from $6 to $24 per cubic meter. Brine

[1] Brackish ground water is defined as water with salt levels over 500 mg/L, or a Total Dissolved Solids (TDS) over 500 ppm.

[2] Throughout the report water volume will be expressed in cubic meters and water costs in dollars per cubic meter. One acre-foot equals 1233 cubic meters, and one cubic meter equals 264 gallons .

disposal increases the blended price for water provided by inland RO to between $0.95 to $2.75 per cubic meter—a price well beyond the $0.60 per cubic meter that growers of even high value crops (e.g., vineyards, tree nuts, tomatoes, berries) can afford.

Why is brine disposal so expensive? Weight of the brine is the key issue. An RO facility treating 100 acre-feet of brackish water at 90% recovery will leave 10 acre-feet, 13,600 tons of brine to be disposed. The four environmentally approved disposal means now available – (1) transportation to an ocean disposal point, (2) injection into a deep well, (3) evaporation in a surface pond, and (4) evaporation in a dedicated thermal Zero Liquid Discharge (ZLD) facility—are all far too expensive.

Of these four disposal methods the one for which technology advances could dramatically lower disposal cost is the dedicated ZLD facility.

Status at the End of Phase I

Phase I work addressed the need for a ZLD system that treated the waste brine discharged from an inland RO facility for brackish water. Similar to commercially available technology, this ZLD system will have two stages: (1) a brine concentrator and (2) a brine crystallizer. These two components face very different challenges.

The Phase I work targeted an agricultural application where an RO first-stage converts 85% to 90% of a brackish water feed to essentially mineral-free water. In this application the RO waste brine to be treated by the ZLD system still has a fairly low mineral concentration—on the order of 10,000 to 30,000 ppm TDS. However, although the TDS is low the brine is saturated or nearly saturated with several mineral salts. These "sparingly soluble" salts, which include $CaSO_4$, $NaSO_4$, $Mg(OH)_2$, will precipitate and foul heat transfer surfaces and flow passages when water is separated from the brine. Further complicating the fouling problem is the fact that these sparingly soluble salts are "reverse soluble", i.e., their solubility in water decreases at higher temperatures.

The brine concentrator must extract water from the brine under conditions where the sparingly soluble salts precipitate. This extraction proceeds in the concentrator until a second critical limit is reached: the concentrations of "highly soluble" salts, such as NaCl, $MgCl_2$, and $CaCl_2$, become very high. Brine discharged from the concentrator might have TDS levels on the order of 200,000 ppm with highly soluble salts being the dominant species.

For thermal separation processes high concentrations of highly soluble salts create two problems: (1) salt concentrations can exceed saturation and the salts can precipitate, and (2) the salts, which form bonds with the water molecules in solution, suppress the pressure of water vapor in equilibrium with the brine (i.e., the salt produces a Boiling Point Elevation—BPE). Since thermal separation relies on fluxes of water vapor that are driven by vapor pressure differences, any effect that suppresses the brine's equilibrium water vapor pressure (which is equivalent to increasing the brine's BPE) will adversely affect the process. The brine crystallizer must then work under conditions where highly saturated salts precipitate and the brine has a high BPE.

Brine Concentrator

The proposed technology for the brine concentrator is an advanced implementation of AILR's proven, patented[3] Diffusion-Gap Distillation (DGD) process for seawater and brackish water. DGD achieves high efficiencies and distillation fluxes by locating hot surfaces that are wetted with evaporating brine close to cooled surfaces that condense the evaporated water vapor—the gap between the two surfaces being between 2.5 mm and 3.5 mm (0.10 to 0.14 inch). Since DGD operates at atmospheric pressure, the gap between surfaces is filled with a mixture of water vapor and air. However, the small size of the gaps allows a small temperature difference between the two surfaces to drive a relatively high flux of water vapor. Since the heat/mass transfer surfaces in a DGD system are either plastic or fiberglass (as opposed to the titanium and high nickel alloys used in conventional brine concentrators) high efficiency is achieved in a compact and low-cost system.

As shown in Figure 1, the key features of DGD are (1) thin, flat, hollow, plastic plates within which the feed brine flows upward, (2) flat, non-woven fiberglass wicks positioned in the gaps between the plates on which the hot brine flows downward, (3) a source of thermal energy, shown in Figure 2 as atmospheric pressure steam—but which can be a heat exchanger with an external source of thermal energy—which heats the preheated brine before it is distributed to the top of the wicks, and (4) condensate films that form on the exterior surfaces of the vertical plates, the heat released as water vapor condenses in these films preheating the brine flowing upward within the plates. (The DGD process is illustrated in Figure 1 with only two plates. Practical systems will typically have several hundred plates.)

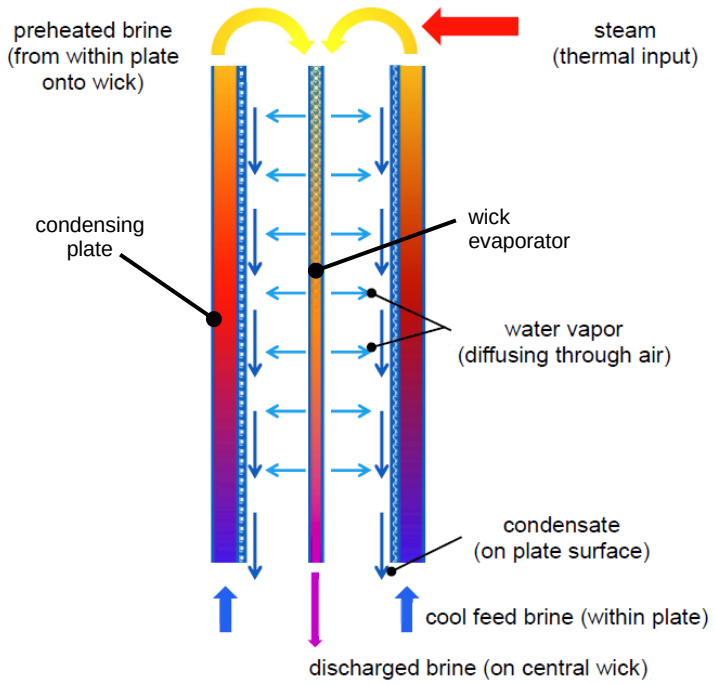

Figure 1 – The Operation of Diffusion-Gap Distillation

The efficiency of the DGD process depends upon the temperature difference across the gap between the evaporating and condensing surfaces. Since the flux of water vapor (kg/s-m2) across the gap is driven by the difference in vapor pressure and ionic salts depress the equilibrium water vapor pressure of solutions, the DGD process will be less efficient when separating water from brine with high salt concentrations.

[3] Lowenstein, "Apparatus for Diffusion-Gap Thermal Desalination,"U.S. Patent No. 9,770,673, Sept. 2017.

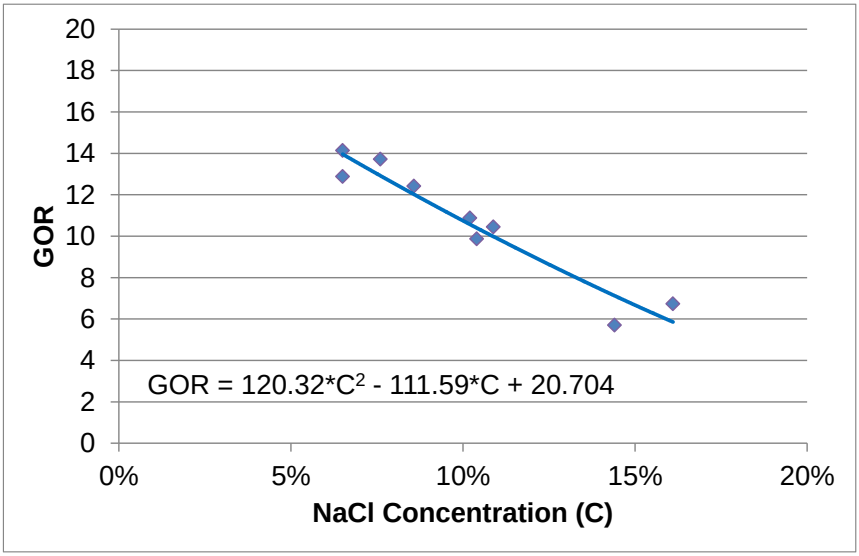

Figure 2 – Dependence of GOR on NaCl Concentration

Figure 2 presents the curve of Gain Output Ratio[4] (GOR) versus salt concentration for the laboratory operation of a DGD model that processes solutions of sodium chloride. As shown in this figure, the GOR for the DGD process decreases from 13.5 to 10.7 to 9.0 as the salt concentration increases from 7% to 10% to 12%. This degradation of GOR is caused by the brine's increasing BPE, which are 2.2°C, 3.1°C and 3.8°C for the preceding three salt concentrations.

In Phase I, we adapted the DGD technology to a brine concentrator that would be the first stage of a ZLD system. As previously explained, the brine concentrator must operate with sparingly soluble salts continually precipitating. The modification to the DGD shown in Figure 3 is designed to handle this operating condition.

As shown in Figure 3, a DGD brine concentrator has a precipitation tank where essentially all crystallization of sparingly soluble salts occurs. The brine feed to the concentrator is saturated with sparingly soluble salts at an inlet temperature close to 20°C. As the brine flows upward within the DGD plates it is heated by the water vapor that condenses on the outside of the plates. As previously explained, the sparingly soluble salts in the brine are reverse soluble—they will become supersaturated as the brine's temperature increases beyond about 60°C.

Although the upward flowing brine within the DGD plates becomes supersaturated, precipitation of salt within the plates will not immediately happen. Changes of phase (e.g., the formation of ice, the boiling of water, as well as the crystallization of salt) can be difficult to initiate. Typically, in the absence of a nucleation site, salt precipitation will not occur until the solution has a high degree of supersaturation. Furthermore, the kinetics of precipitation can be slow so even when nucleation sites are available, crystals will grow slowly.

[4] For a thermal separation process, the GOR is the ratio of the mass of product water divided by the mass of steam that drives the process.

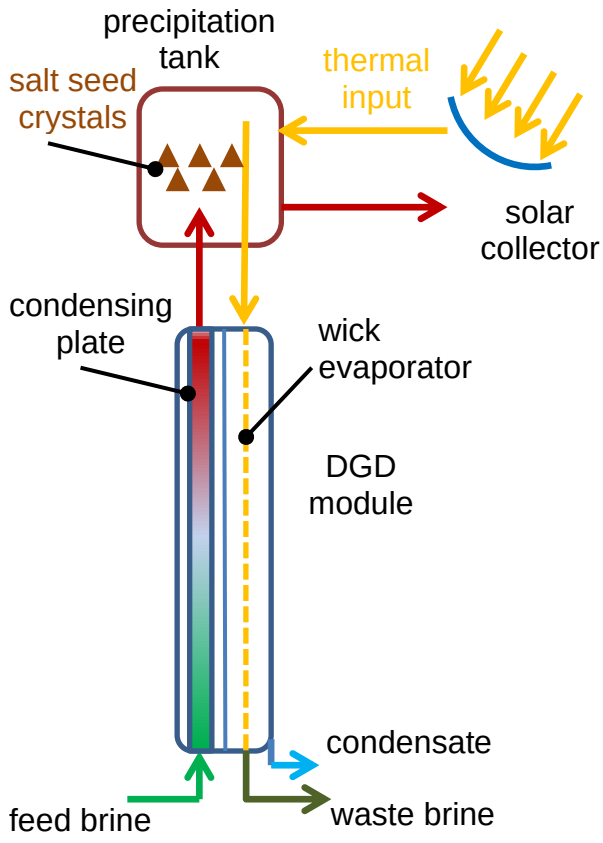

Figure 3 – DGD modified to operate with sparingly soluble salts

The modification to the DGD process shown in Figure 3 exploits the latency period for phase changes and their finite growth rates to direct essentially all salt precipitation to a tank that both has salt seed crystals (i.e., nucleation sites) and provides the supersaturated brine with a long residence time in contact with the seed crystals (i.e. 5 minutes or longer).

An external source of thermal energy heats the brine in the precipitation tank to the system's maximum temperature (i.e., on the order of 100ºC). Upon leaving the tank, the brine is saturated with sparingly soluble salts. As the hot brine flows down the wicks, the brine both cools, which decreases its level of saturation, and evaporates water, which increases its level of saturation. The net effect of these two processes is a decrease of the brine's level of saturation as it flows down the wick that avoids salt formation on the wick.

A one-gap DGD model that processes a saturated solution of $CaSO_4$ (the sparingly soluble salt that is expected to cause the most severe scaling problems) was built and tested in Phase I. Two duration tests were completed—one 54-hour test and one 94-hour test. Both tests ran with no operational problems. Post-test inspections of the wick and transfer lines did not uncover any meaningful accumulation of solid $CaSO_4$. In the 94-hour test, 11.3 kg of pure water (average conductivity typically less than 10 microS) was separated from the brine. Assuming the feed brine was saturated with $CaSO_4$ at room temperature, 27.2 g of anhydrous $CaSO_4$ should have precipitated. The weight change of the $CaSO_4$ seed granules in the precipitation tank was within 2% of this calculated value.

The measured performance of the DGD model during the 94-hour test agreed closely with the performance predicted by our computer model. Figure 4 shows the ratio of experimental and theoretical values for distillate production and GOR. Each data point is an average over six hours. Except for the last three data points, all ratios are in the range of 0.92 and 1.15[5]. This good agreement between theory and experiment allows us to predict the performance of commercial scale systems.

[5] The last three data point are outside this range, but we believe a measurement error led to both the unusually high and unusually low values. The average of the last three data points fall within the 0.92 to 1.15 range.

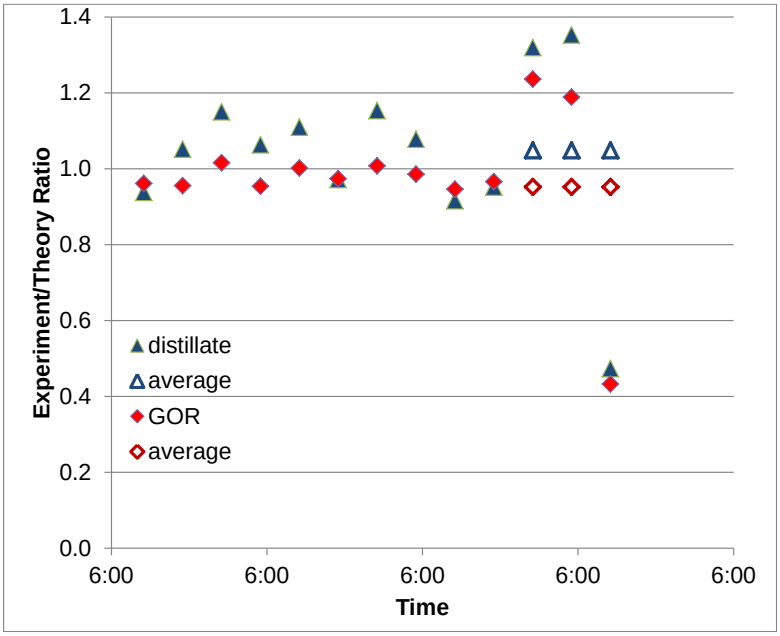

Figure 4 – Comparison of Experimental and Theoretical Performance

Conclusions from Phase I

In Phase I, concepts for both a brine concentrator and brine crystallizer successfully operated in critical proof-of-concept tests. Both concepts operated with salt continuously precipitating and collecting in tanks or sumps where the solids could be removed without interfering with the system's operation. Both concepts also operated with condensate continuously collected with no brine contamination.

The Phase I work was able to circumvent problems caused by salt precipitation through a two-stage process that first precipitates most sparingly soluble salts and then in a second stage precipitates the large load of highly soluble salts. Precipitation of salt does occur as water is extracted in the second stage, but the evaporating surfaces have a coating that prevents salt from accumulating on them.

Primary Objectives for Phase II

At the highest level, the technical objective for the Phase II work is to prove a commercially ready design for a waste brine treatment technology that will begin to open the large market that has been identified for agricultural water in California and throughout the Southwest. This Phase II objective can be met through an R&D effort that develops a manufacturable design for the concentrator's evaporator/condenser plate pair while in parallel explores design/coating options for the crystallizer's plate pair.

Although by itself a brine concentrator is not a ZLD solution to the inland disposal of waste brine, it does provide sufficient value to become a stand-alone treatment system. As previously noted, a brine concentrator will typically reduce the volume of waste brine from a brackish-water RO or EDR facility by a factor of 20. With this reduction in volume final disposal options such as evaporation ponds and trucking to a central facility, while not ideal, will be acceptable to some growers.

The critical Phase II challenge for introducing a commercially viable brine concentration is to scale up the Phase I proof-of-concept model to the size needed to achieve a market-accepted cost for brine disposal. The Phase I model proved performance at a very limited scale: the DGD process occurred in one pair of condensing and evaporating plates with an active area that was 3.5" (W) x 46" (L). A preliminary design for a commercial 5-gpm brine concentrator that ships in a standard 40-foot container will have condensing and evaporating plates with active areas that are 18" (W) x 90" (L). Furthermore, the Phase I model with one active gap must be scaled up in Phase II to a module with at least 60 active gaps.

Phase II Accomplishments

Phase II work, while not yet proving the long-term operation of a full-scale, brine concentrator module, has successfully identified critical failure mechanisms. All identified failure mechanisms have reasonable design solutions that are now being implemented in a 30-plate model with full-size plates (i.e., 18" x 90").

If a DGD brine concentrator is to expand inland water resources it must meet an initial cost metric of $3.40 per cubic meter of processed brine. The CAPEX for the DGD, which will be on the order of $2.00 per cubic meter, can be met only if the central processing module is fabricated from relatively inexpensive materials. The extruded polypropylene condensing plates and non-

woven fiberglass wicks that were successfully used in the Phase I work can meet the target CAPEX for a commercial system.

The design for a DGD prototype composed mostly of extruded polypropylene plates and non-woven fiberglass wicks that can efficiently operate long term must address the following challenges:

1) During the start-up transient, the upper section of the prototype increases in temperature by approximately 80^{o}C (144^{o}F). The Coefficient of Thermal Expansion (CTE) for the polypropylene plates is about an order of magnitude greater than the CTE for fiberglass. This difference in expansion/contraction during thermal cycling must be accommodated without stress-induced distortions that cause the brine wicks and condensing plates to touch.
2) The scale-up of the prototype to plates that are approximately 8 feet (2.4 m) in height greatly increases that hydrostatic pressure on the fittings and seals at the bottom of each plate.
3) The scale-up to longer plates must be accompanied by a higher brine flow per wick if the CAPEX target is to be met. The requirement to collect the brine that flows off the wicks without contaminating the condensate that flows off the plates becomes more difficult to meet as the per-wick brine flow increases.
4) Polypropylene is a mostly non-crystalline material that creeps under stress. The creep will be greatest at high temperature and can lead to distortions that compromise critical isolation/sealing elements within the assembly.

Four DGD prototype were built and tested during the first year of the Phase II work. The Year I work, which was reported in the project's first interim report, is again reported here.

During the second year, eight additional configurations were built and tested. Although none of the twelve designs achieved long-term, reliable operation, failure mechanisms associated with both the wicking surfaces and condensing plates were identified. Following a description of the operating experience with the second-year designs, a thirteenth design is described that addresses the identified weakness and failure mechanisms.

Design 1—August 2019 Tests

The first model to be tested had five condensing plates with four wicks positioned in the gaps between the plates. Key features of this first design were:

1) The non-woven fiberglass wicks were applied to a thin G-10 substrate. Surface tension between the wetted wicks and the G-10 substrate was the only mechanism for holding the wicks flat on the substrate.
2) The wicks/substrates and the condensing plates were hung from a steel frame within an insulated enclosure
3) A U-shaped polycarbonate gutter was attached to the bottom of each G-10 substrate. The gutter collected the brine that flowed off the wicks and directed the brine to a collection trough located next to the five-plate assembly

Three tests were conducted on the first model, the longest test starting on August 14 and lasted approximately 24 hours. The test was stopped when data showed unacceptable heat loss from within the insulated enclosure (i.e., the temperature of the brine discharged from the bottom of the wicks was cooler than the brine feed to the bottom of the condensing plates.)

A post-test inspection showed that the steam within the insulated enclosure had warped the epoxy-coated insulation panel that was the enclosure's top. This warping created an air/vapor leak from the enclosure.

The post-test inspection also showed several problems in the model's design. The G-10 substrate for the wicks had warped in a way that cupped the substrate. Furthermore, the non-woven fiberglass wicks did not stay flat against the G-10 straight but rather puckered into a pattern of bumps and ridges. The combination of the cupped substrate and puckered wicks brought several wicks in contact with their neighboring condensing plates leading to contamination of the condensate (i.e., the conductivity of the brine collected by the individual gutters ranged from an acceptable 42 microS/cm to an unacceptable 248 microS/cm).

Design 2 – October 2019 Tests

The most significant problems with Design 1—cupping of the G-10 substrate and separation of the wick from the G-10 substrate—were addressed in Design 2 by replacing the G-10 substrate with a 1/16" thick sheet of polypropylene. This switch to polypropylene allowed the non-woven fiberglass wicks to be spot welded to the substrate (an approximately 2" x 2" pattern of spot welds). Since the polypropylene sheet was not as flat as the G-10 (as received from the vendor), a series of rivet-spacers were attached to the wicks/substrates in a 6" x 6" pattern. The rivet/spacers were 3-D printed to have a height that matched the gap between the condensing plate and the wicks.

The five-plate/four-wick assembly was again hung from a steel frame within the insulated enclosure. Gutters where again attached to the bottom of the wicks, but the polycarbonate gutters

were replaced with an assembly composed of a 3-D printed plastic base for collecting condensate and an aluminum extrusion upper section for collecting brine.

The Design 2 model could not be tested at design temperature. A post-test inspection showed that the spot-welds for the non-woven fiberglass broke during heat up of the model as the poly-propylene substrate expanded in length. Once the welds were broken the wicks detached from the substrate and contacted the condensing surfaces. Post inspection also showed significant warping of the polypropylene substrate in the unconstrained spans between the rivet/spacers.

Design 3 – November 2019

Design 3 incorporated two major modifications to Design 2. The substrate for the non-woven fiberglass wicks was changed to the same 2-mm polypropylene profile board manufactured by Coroplast that is used for the condensing plates. The tests of the Design 1 and Design 2 models had shown the geometry of the condensing plates to be stable. i.e., unlike the G-10 and the 1/16" polypropylene substrates the condensing plates remained flat after days of operation.

The second modification changed the approach to supporting the multi-plate assembly. Instead of tightly compressing the assembly at the top and then hanging it from a frame so that it could expand downward as it heated up, the assembly was tightly compressed at the bottom and then mounted on a base so that it could expand upward. This change shifts the highest stresses on the polypropylene plates from the hotter upper region (where the plates were in tension) to the cooler lower region (where the plates are in compression).

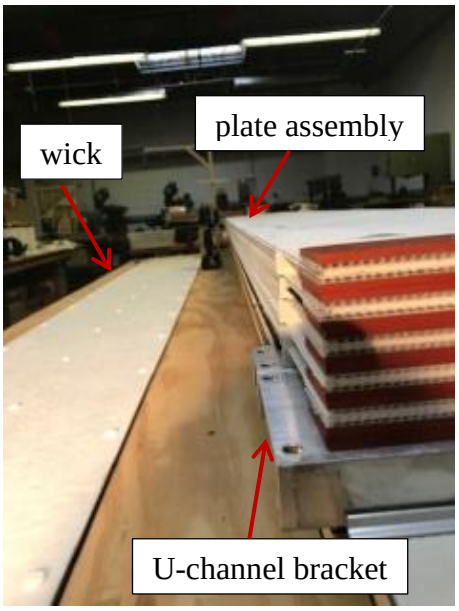

Figure 8 – Design 3 Assembly of Five Plates

Rivet/spacers were again used in Design 3 to maintain the gap between the condensing plates and the wicks. The gutters used in Design 2 were again used in Design 3.

Figure 8 shows the five-plate assembly of condensing plates for Design 3 next to one of its wicks. The red silicone sheets shown in this figure form the seals that create a brine inlet manifold internal to the assembly. The plate assembly is shown sitting on one of the two aluminum U-channel brackets that compress the stack assuring that the silicone seals are leak tight.

Figure 9 shows the Design 3 assembly set up for testing.

The Design 3 model started to process a 7% solution of NaCl on November 29, 2019 at 11:20 am and was turned off at 2:30 pm on Dec 3, 2019. During the four-day test the model did not deliver condensate of acceptable purity. However, temperature measurement of the brine into and out of the condensing plates confirmed

that the model's thermal performance was good, i.e., condensation on the outside of the condensing plates was providing the expected amount of brine preheating. For example, during a 100-minute period starting at 4:20 am on December 3, the measurement of brine temperatures into the condensing plates, out of the condensing plates and onto the wicks indicated a Gain Output Ratio (GOR) of 10.3. Computer modeling of the operating conditions during this 100-minute interval predict a GOR of 12.4.

Figure 9 – Design 3 Assembly under Test

Although the computer model predicts a 17% higher efficiency, a GOR over 10 when processing 7% NaCl is good for a processor with only five plates.

The test of the Design 3 model showed the gutter collection of brine to be problematic. We suspect that the gutters were not staying centered and vertical within the gaps between condensing plates. The slightly angled positioning of the gutters brought the lips of the gutters in contact with the condensing plates at one or more locations, which then produced crossover of brine from the gutter to the condensate.

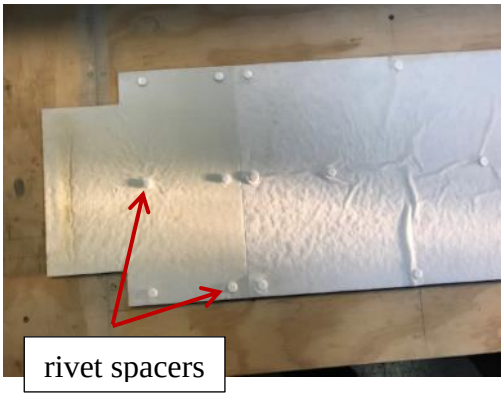

Figure 10 – Wick Plate for Design 3 after Four Days of Testing

The wicks for the Design 3 model were made in two parts. The upper 8" section of the wick, which operates exposed to the hottest brine, is a non-woven fiberglass that has a binder designed for high temperature operation. The lower 88" section of wick is a less expensive non-woven fiberglass with a binder not designed for high temperature operation.

As shown in Figure 10 the wick with the high temperature binder (i.e., the slightly yellowed wick at the left end of the plate) remained flat while the lower section of wick puckered during the thermally cycling of the model. (The rivet/spacers are shown in this figure.)

Design 4 – March 2020

The poor collection performance of the gutters that were attached to the bottoms of the wicks in Design 3 led to a major revision of the condensing plates. As previously described, the Design 3 model had an internal brine manifold that was formed by a combination of silicone rubber seals and cutouts within the plates. This approach to delivering brine to internal passages of the plates is shown in Figure 11a.

Since the silicone rubber seals in Design 3 (shown in red in Figure 11a) fill the gaps between the condensing plates, all brine and condensate must be collected above the seals. This need was met by attaching U-shaped gutters at the bottom edges of the wick substrates. The brine that flowed off the wicks flowed into the gutters which then carried the brine to the side of the plate assembly.

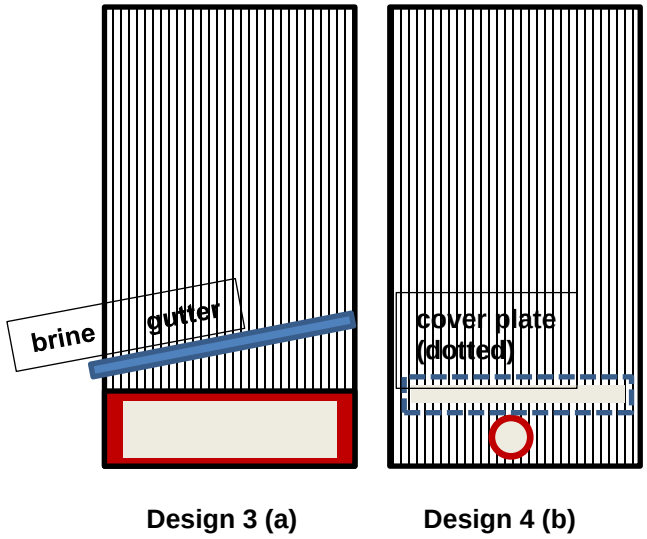

Figure 11 – Delivery of Brine to the Internal Channels of a Condensing Plate

The fluid collection approach implemented in Design 4 extends the wicks and their substrates downward to the bottom edge of the condensing plates. With the bottom edges of both the condensing plates and the wick substrates lying in the same plane, a grooved collection pan with each plate and substrate standing in its own groove collects the condensate with no contamination from the brine.

The preceding approach to fluid collection requires a brine supply manifold that does not interfere with the extended wicks and their substrates. As shown in Figure 11b, the new brine supply manifold for Design 4 has two features: (1) relatively small circular openings in the bottom of each condensing plate that form a continuous internal manifold when plates are stacked with O-ring silicone gaskets (red circles in Figure 11b) between plates, (2) rectangular cutouts in the condensing plates that receive brine from the circular internal manifold and distributes the brine laterally to all the internal passages of the plate. Thin cover plates are bonded over the rectangular cutouts to contain the brine.

Another important difference between Designs 3 and 4 was the elimination of rivet/spacers for maintaining the gap between the wicks and the condensing plates. Instead of rivet/spacers, three continuous ribs were inserted in the gaps. The ribs were narrow (about 4 mm wide) and positioned at each outboard edge of the plates and along the vertical center line. The wicks were made entirely from non-woven fiberglass with high temperature binder, and they were tacked to the surface of the substrate with a high temperature contact adhesive. (Prior to assembling the wicks/substrates sample coupons were exposed to a 95^{o}C steam environment. No significant changes to the coupons were observed after more than two weeks of exposure.)

The final significant change for the Design 4 model was to increase the number of condensing plates from five to ten. The larger number of plates allowed a more meaningful projection of performance for a full-scale module since “end effects” are less important in the ten-plate model.

Figure 12a – Photographs of Design 4 Model

Figure 12b – Photographs of Design 4 Model

Figures 12a and 12b show photographs of the fabrication of the Design 4 model and its set-up within the support frame.

Figure 13 shows the data for the operation of the Design 4 model processing 7% NaCl during a 24-hour test that began at 10:30 am on March 20, 2020. The data in this figure show normal operation until about 6:00 pm. During this period of normal operation, the brine is preheated as it flows upward within the condensing plates to within about 10°F of the temperature of the brine that delivered to the top of the wicks (i.e., the temperature difference between the red and blue traces in Figure 12). However, after 6 pm, the temperature difference between the red and blue traces diverges, slowly at first but at an accelerated rate after 9:00 pm.

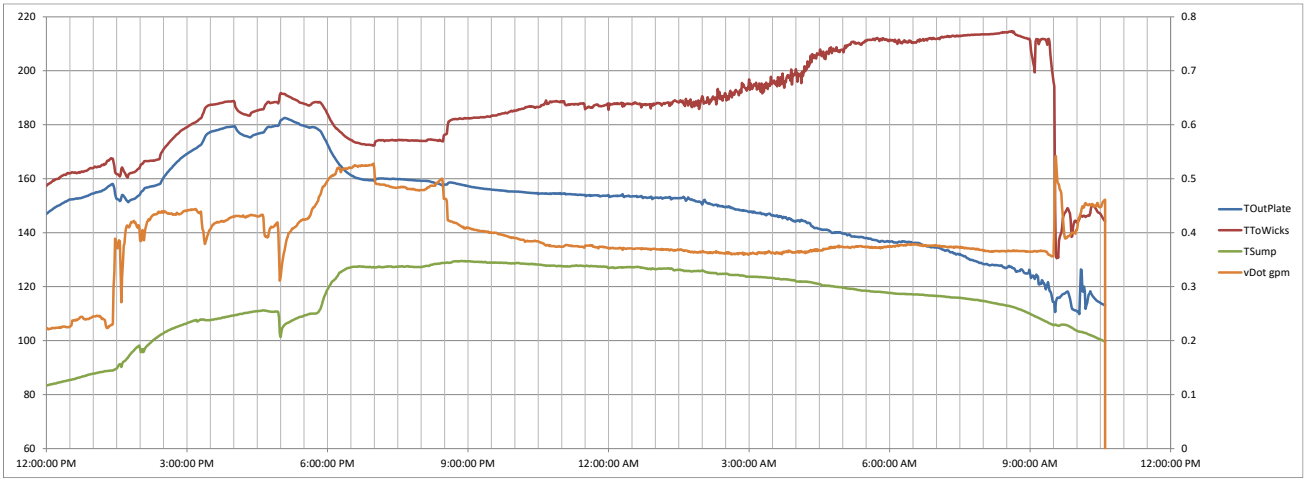

Figure 13 – Performance Data for March 2020 Test of Design 4 Model

During the 30-minute period between 3:30 pm and 4:00 pm, the Design 4 model operated at a 8.3 GOR (based on the measured temperatures of the brine). This GOR is about 10% lower than the 9.2 value predicted by our computer model of the DGD process.

A post-test inspection of the Design 4 model revealed two locations where the thin plates that cover the rectangular cutouts in the condensing plates (see Figure 11b) had failed under the pressure of the brine.

Design 5 – May/June 2020

Three alternate approaches to sealing the rectangular cutouts in the condensing plates were implemented in sub-scale coupons that could be pressurized with air. A fourth coupon was prepared using the same approach to sealing that was used in Design 4. All coupons held pressure when pressurized to 150% of nominal operation (i.e., 6 psi vs 4 psi) for 48 hours. Following this initial pressurization, pressure was slowly increased at a rate of about 2 psi per 10 minutes. The coupon with the Design 4 approach to sealing failed at about 12 psi. The other three coupons held pressure at the air pump's maximum output of 24 psi.

A ten-plate Design 5 model was assembled that used the approach to sealing the lower rectangular cutouts that withstood a pressure six times nominal operating pressure.

The Design 5 model began operation in May 2020. After thermally cycling the model several times it was noted that several of the condensing plates had shrunk in length by approximately 1/8". This shrinkage is shown in Figure 14.

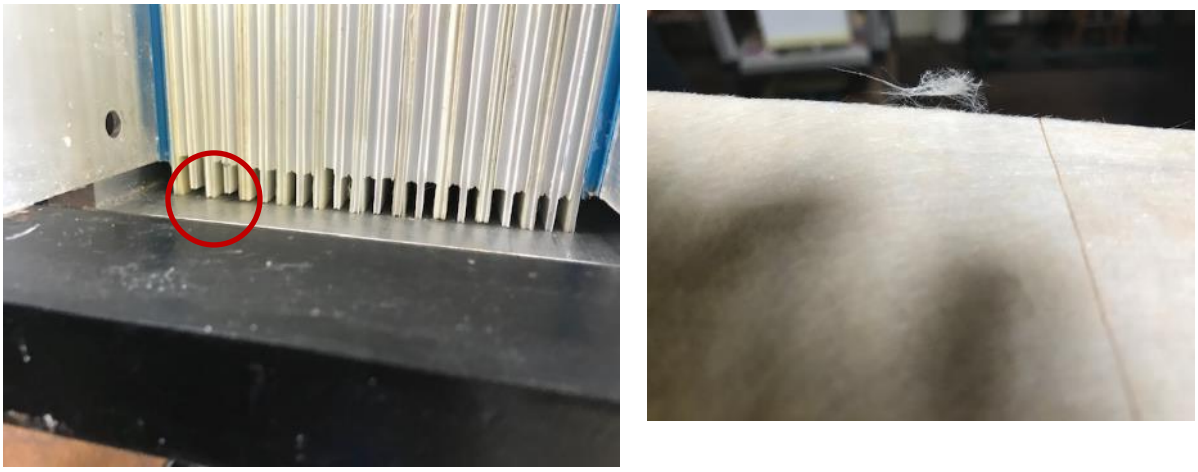

a) Shrinkage of condensing plates **b) Failure of non-woven fiberglass wicks**

Figure 14 – Post-Test Photographs of Design 5

Attempts to operate the Design 5 model failed when significant amounts of brine were detected in the condensate collection troughs prior to applying heat. A post-test inspection of the model showed that the fiberglass wicks, which were bonded with a high temperature contact cement to 2-mm Coroplast plates, were detaching (see Figure 14 b).

Design 6 – September 2020

A fundamental problem with bonding fiberglass wicks to Coroplast plates is that the Coroplast has a much higher Coefficient of Thermal Expansion (CTE) than the fiberglass. In Design 5, the stresses cause by the difference in CTEs was minimized by slitting the fiberglass wicks in the hottest zones (upper 12") into 4" squares. Although this approach appeared to be effective, it is a labor-intensive operation.

During a visit by a representative from the Inteplast Group (the parent company of Coroplast), we were provided samples of 2-mm Coroplast with a thin polyester fabric laminated to the plate surface. In brine flow tests the fabric-covered samples proved sufficiently porous to carry the required brine flow without rivuleting (i.e., the brine flowed within the pores of the fabric and did not form narrow streams flowing outside of the fabric).

With minor modification to Design 5, the most significant modification being the replacement of the fiberglass wicks with fabric wicks, a new 10-plate model was constructed (Design 6). Figure 15 shows two photographs of the Design 6 model under construction.

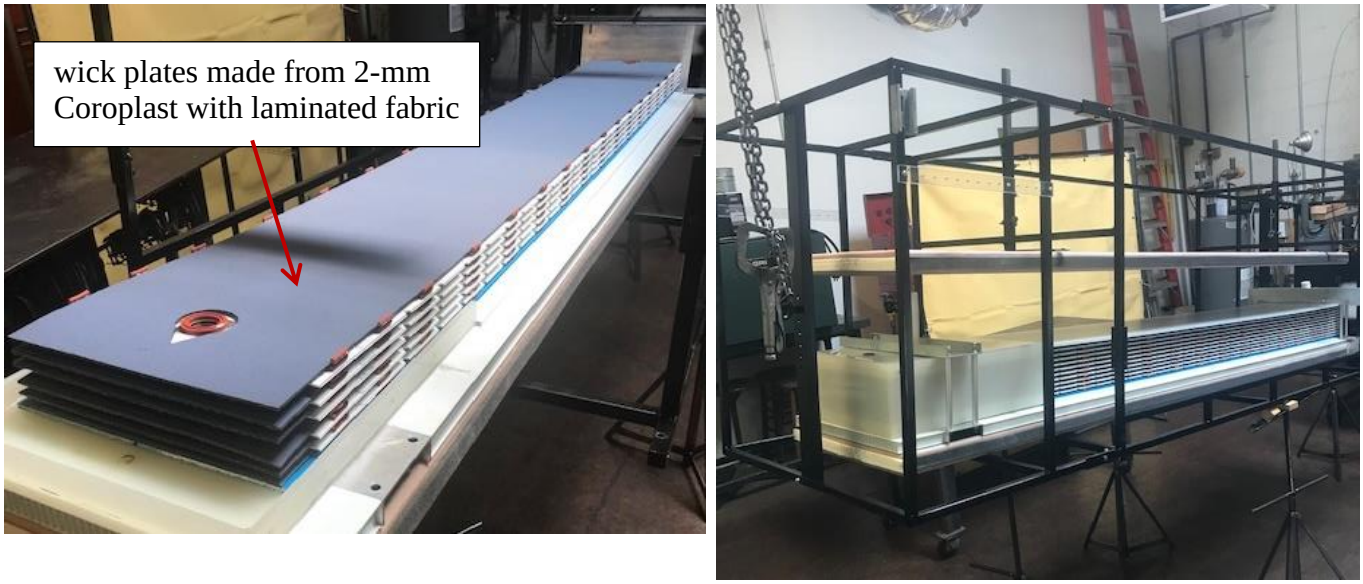

Figure 15 – Assembly of Design 6 Model

Figure 16 – Post-Test Inspection of Design 6 Model

Starting on September 3, 2020, Design 6 processed 7% NaCl continuously for approximately one week. The temperature of the brine delivered to the wicks stayed mostly in the range between 77°C and 84°C. The brine flow was approximately 0.25 gpm (about 60% of the nominal design flow).

Initial operation was good with product condensate having a low conductivity (i.e., between 20 and 30 microS/cm during the first two days of operation). After five days of operation, condensate conductivity rose to 60 microS/cm. Measured GOR for Design 6 operation was lower than expected, i.e., about 80% of the values predicted by our EES computer simulation of the DGD process.

Following the one-week test, the 10-plate Design 5 model was disassembled. Post-test examination uncovered several severe degradations that clearly compromised performance. As shown in the left photograph in Figure 16, the fabric delaminated at several locations in the hottest regions of the wick plates (i.e., the region under the distribution sponges (yellow elements in Figure 16) that receive the hottest brine).

A second severe degradation was the buckling of both the condensing plates and wicking plates, which is shown in the right photograph in Figure 16. This buckling is attributed to the compressive stresses imposed on plates that stand on their bottom edges. We had anticipated that the plates might buckle when exposed to high temperatures for long operating periods and had clamped the plate stack between rigid sidewalls with spacers maintaining the gaps between wicking plates and condensing plates. However, the rigid sidewalls only lightly compressed the stack of plates to allow for thermal expansion during operation. The post inspection revealed that light compression of the stack was not sufficient to prevent buckling.

Design 7 – December 2020

To address problems encountered in the operation of the Design 6 model, a seventh model was fabricated with the following changes:

- The fabric-covered 2-mm plates, which delaminated during high temperature operation, were replaced with 2-mm plates covered with sleeves made from knitted nylon fabric. (The knitted fabric stretches both vertically and horizontally and so should not create stresses due to differential thermal expansion). The sleeves were sized so that they were slightly stretched when slipped over the plate. As an added precaution against the wicks separating from the plates, the sleeves were sewn to the plates at three spaced-apart seams running almost the entire length of the plates. Delamination or bubbling of the wick, which was observed with the laminated fabric wicks and the adhered fiberglass wicks (Design 5), should be avoided in this design.
- The wicking plates were hung by clamping their topmost edges between small silicone-rubber pads that were bonded to the upper cover plates of the condensing plates. The

lower edges of the wicking plates are contained within grooves in the base plate that separately collected the brine and the condensate, but the lower edges are about ½" above the bottom of the groove (so the wicking plates hang in tension to prevent buckling).

- The condensing plates again stand in the grooves of the base plate, but "comb" spacers were added at the edge of the plates to maintain uniform spacing.

The performance of the Design 7 model was disappointing in that low conductivity condensate was never produced. During operation, bubbles were observed to form and break in the grooves that collected the brine that ran off the wick plates. This bubbling was caused by a passive pumping of brine within the flutes of the 2-mm Coroplast wick plates. With the walls of the wicking plates pierced when the sleeves were sewn onto the plates, openings were created where a mixture of air and brine could enter the flutes. The mixture could flow downward under gravity and exit the flutes at the bottom of the plates. Brine bubbles formed and broke as the brine and air exited the flutes. With the condensate collection grooves separated from the brine grooves only by a thin wall the bursting bubbles contaminated the condensate.

The bursting brine bubbles were not the only problem with Design 7. Post inspection after approximately eight days of operation showed severe buckling of the plate stack that caused contact and fluid crossover between condensing plates and wick plates (See Figure 18).

Design 8 – March 2021

The two major problems encountered with the Design 7 model were address in the Design 8 model by the following modifications:

- The bubbling problem caused by the requirement to sew a knitted fabric to the 2-mm Coroplast plate was eliminated by flocking a dense layer of 20-mil nylon fibers to the surfaces of the wick plates. Flocking of the plates was performed by EIS Fibercoating (Logansport, IN). Samples of flocked plates were first received and exposed to 100^{o}C steam for several days. With no apparent change in the exposed samples, a full set of plates, shown in Figure 19, was prepared by EIS Fibercoating.
- To reduce the buckling of the condensing plates, the stack of plates was clamped to a slightly smaller overall width. The reduced "free play" between plates greatly limited the potential for buckling.

A partially assembled stack with flocked wicking plates is shown in Figure 20,

The Design 8, 10-plate model operated in March 2021 for a total of 37 hours, but never produced low conductivity condensate. One problem was caused by flock fibers that were only loosely bonded to the plates. These loose fibers washed down the plates and, as shown in Figure 21, formed clumps at the bottom of the condensing plate. These fiber clumps created paths for brine to flow from the wicks to the condensing plates.

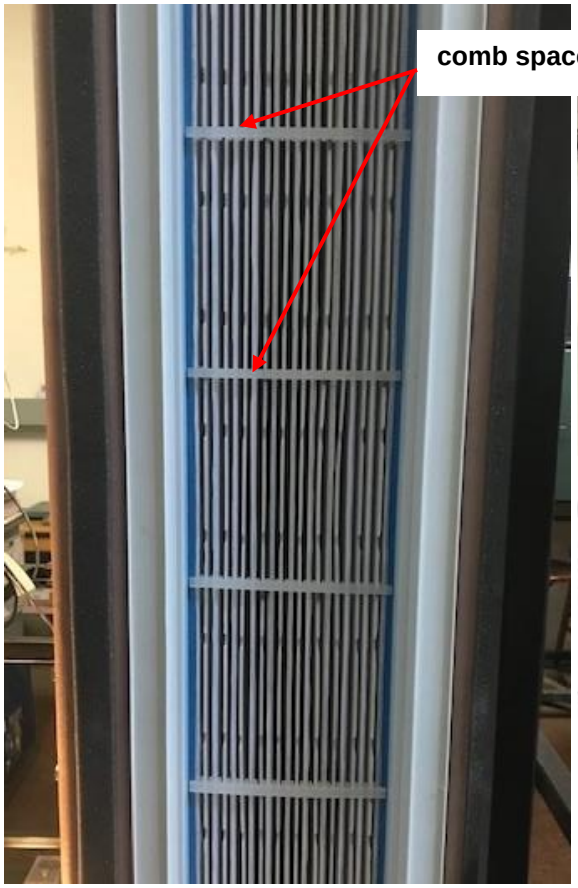

Figure 17 – Assembled Design 7 Model

Figure 18 Post Test Inspection of Design 7 Model

Figure 19 – Flocked Wicking Plates

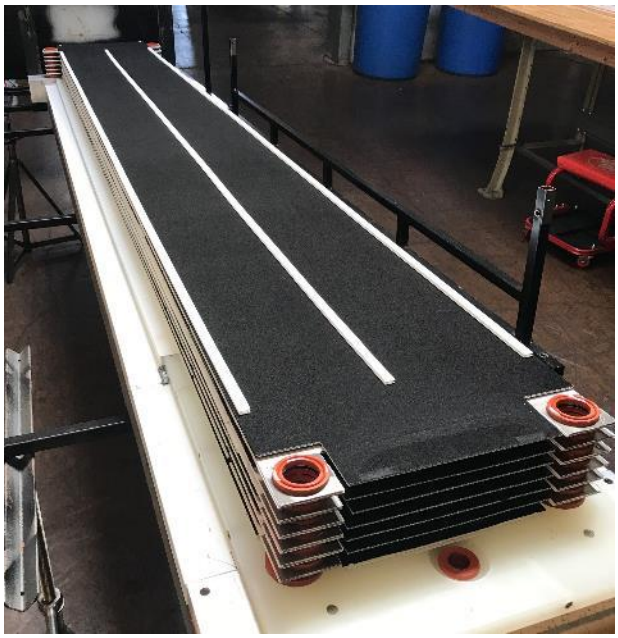

Figure 20 - Partially Assembled Design 8 Model

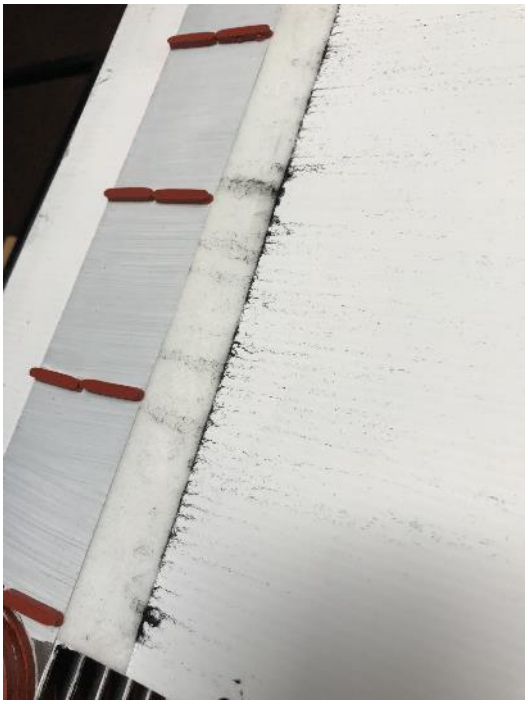

Figure 21 – Accumulation of Loose Flock Fibers

Figure 22 – Bubbling of the Flock Layer

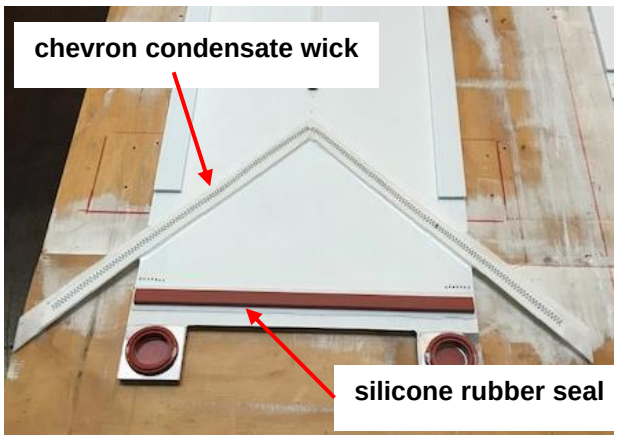

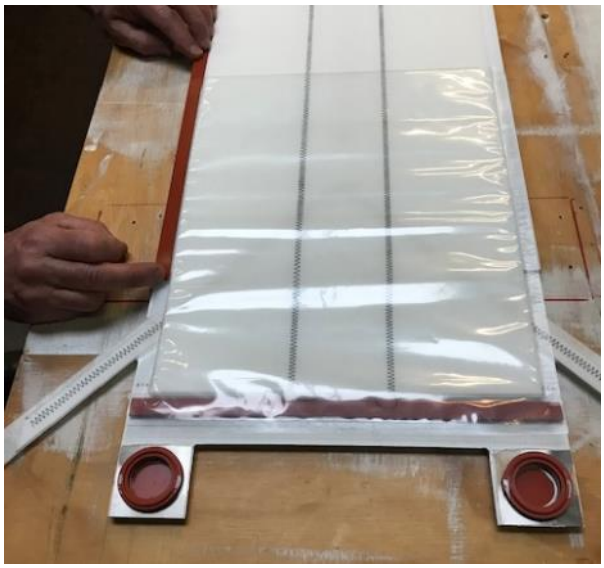

Figure 23 – Design 9 Condensate Collection and Brine/Condensate Isolation

A more severe problem occurred in the high temperature sections of the flocked plates where bubbles formed in the flock layer. This failure mechanism is shown in Figure 22. Both loose fibers and the bubbling could allow brine to cross over to the condensing plates and contaminate the condensate.

Design 9 – July 2021

The Design 9 model incorporated two major changes:

- The 10-plate stack was modified so that the entire assembly hung within the steel frame support structure.
- The wicking plates, which were 2-mm Coroplast plates covered with a wicking layer, were replaced with a simple two-ply sheet of non-woven fiberglass.

In previous designs the individual condensing plates stood in grooves that had been machined in a base plate. The base plate had a second set of interlaced grooves that collected the brine that flowed off the wicking plates.

Maintaining isolation when brine and condensate are collected in neighboring grooves of the base plate proved challenging. In Design 9 the base plate was eliminated and replaced by features that allowed the brine to be collected below the plate stack and the condensate collected outboard of the plate stack.

As shown in the left photograph in Figure 23, Design 9 used chevron-shaped wicks lightly tacked to each surface of the condensing plates to direct condensate outboard of the plate stack. These condensate wicks consisted of three layers of non-woven fiberglass that were sewn together. The condensate that dripped off the ends of the wicks was collected in U-channels outboard of the plate stack.

As shown in the right photo in Figure 23, isolation between the condensate and the brine was maintained by enclosing the brine wicks in thin-film polyethylene bags in the region where the main brine wicks and the chevron condensate wicks overlapped. A narrow rectangular spacer made from silicone rubber, which is shown in both Figure 23 photographs, was bonded the lower cover plate. The thickness of this spacer was sized so it sealed the gap between condensing plates when the plate stack was compressed between aluminum U-channel brackets. The brine wicks with isolation bags ended about ½” above the lower cover plates. The brine that flowed off the brine wick was then diverted by the rectangular spacers to the edges of the condensing plates. Pieces of wicking twine laid in the gap between condensing plates immediately above the rectangular spacers directed the brine to U-channels positioned under the plate stack and inboard of the U-channels that collected condensate.

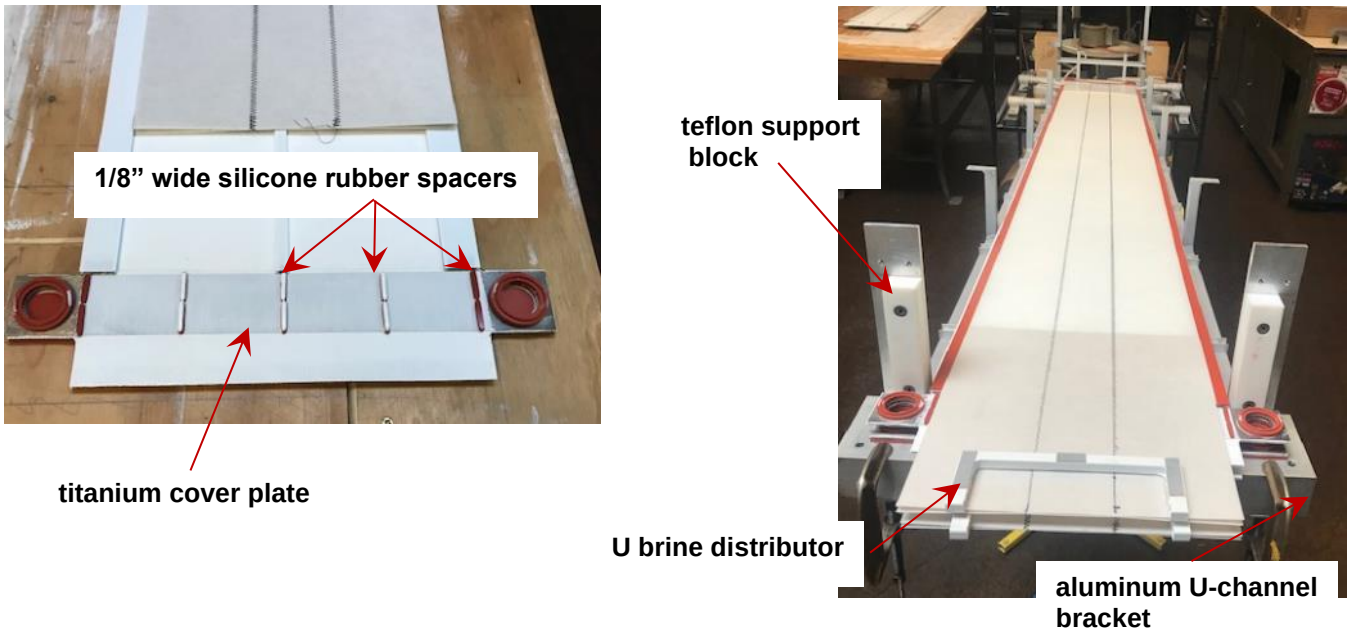

Figure 24 – Design 9 Brine Delivery and Upper Support for Condensing Plates

The top of a condensing plate is shown in the left photograph in Figure 24. As shown in this photograph a 20-mil sheet of titanium that extends 2” beyond the main body of the condensing plate seals the upper cutout in the condensing plate. Silicone O-ring seals are bonded over the circular openings in this cover plate so that a sealed fluid passage is created when the stack of plates is compresses.

Narrow (1/8” wide) pieces of silicone rubber are bonded at five locations along the titanium cover plate. With each brine wick in its final position even with the top of the condensing plates, the three central pieces of silicone rubber, which are slightly thickened with a bead of RTV adhesive, capture the brine wicks when the stack is compressed.

Brine delivery across the top of the brine wicks is provided by the U-distributors shown in the right photograph in Figure 24. These distributors were cut from 10-mm Coroplast and positioned above the condensing plates between wicks. Sections of 1/16” foam tape (grey sections on the white distributor) are bonded to each distributor so that the distributors are fixed in place when the stack is compressed. During operation, a shallow pool of brine forms within the U-distributors and evenly wets the central 8” of the 12” wide brine wick.

A final step in the assembly of the 10-plate stack was to compress the upper region of the stack between a pair of upper aluminum, U-channel brackets. When compressed, the sections of the titanium upper cover plates that extend 2” beyond the central body of the condensing plates

provide a stiff edge from which to hang the assembly on the Teflon support blocks that are part of the steel support frame.

Operation of Design 9 on July 10 was limited to 5 hours under heat due to significant carryover of brine onto the chevron wicks for condensate. Post inspection of the plate stack uncovered three problems:

- Several pairs of the narrow pieces of silicone rubber that press into both sides of each wick were not aligned. This misalignment, which did not create problems when the wicks were attached to 2-mm Coroplast plates, locally distorted several wicks leading to the wicks touching the opposed condensing plates. This contact allowed brine to flow down the condensing plates.
- The top edges of the condensing plates that extend approximately 2" above the upper titanium cover plates distorted under the thermal stresses of heating. This distortion further exacerbated the contact between the wicks and the condensing plates.
- The 10-mm thickness for the U-distributors was slightly oversized causing the top of the wicks to splay outward further exacerbating the wick/plate contact problem.

Design 10 – September 2021

The Design 10 model incorporated two changes that addressed the problems in Design 9:

- The tops of the condensing plates, which had distorted under the stresses of thermal cycling, were trimmed so that they extended only about ¼" above the top edge of the titanium cover plate.
- The central U-distributors were changed to an 8-mm thickness with only the end U-distributors left at 10-mm thickness.

Design 10 operated for 24 hours on September 9/10. Low conductivity condensate was not produced during the run. Post inspection showed that several of the pairs of narrow spacers that captured the tops of the wicks, while they were aligned at the start of the run, had shifted position when the model was heated. This shift misaligned several spacer pairs and sufficiently distorted the top of several wicks to cause them to touch the neighboring condensing plates.

Design 11 – October 2021

Design 11 incorporated two major changes that both addressed the problems observed in Design 10 and simplified the assembly process:

- The approach to hanging the wicks was changed so that the 1/8"-wide spacers on the top cover plates that had captured the top of the wicks were eliminated. The new approach to hanging the wicks relied on the U-channel brackets that compressed the wicks and U-

distributors. With these brackets supported by the frame, the wicks captured by the U-distributors remain fixed relative to the top of the plates.

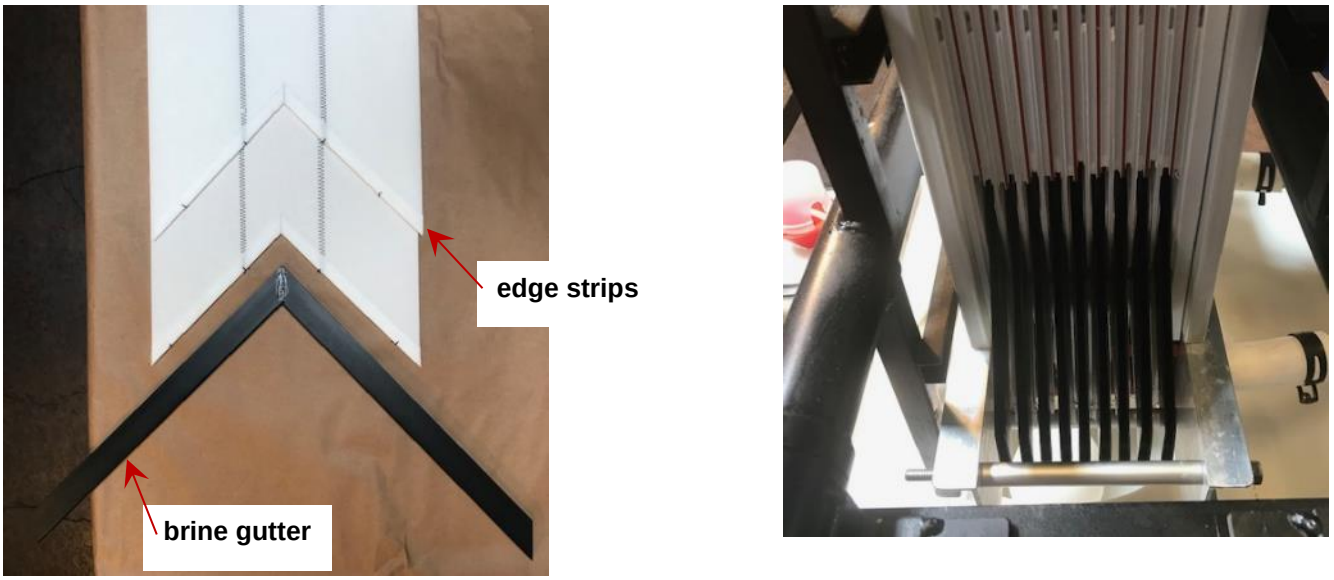

Figure 25 – Design 11 Brine Collection Gutters

- The thin-film bags were replaced as the means of insuring isolation between the lower sections of the wicks and the condensing plates. Instead of the bags, the bottom edges of the wicks were centered in the gap between condensing plates by inserting the edges into chevron-shaped gutters.

The brine gutter shown in Figure 25 is formed from two pieces of U-channel extrusion that is available from SeaGate Plastics. The PVC extrusion has 1" high side walls with a 5-mm inner gap between the side walls. Two pieces of U-channel are glued together at a 90-degree angle to form the chevron gutter.

Chevron-shaped strips of 30-mil nonwoven fiberglass that are slightly wider than the gutter side wall height are lightly bonded to the faces of the condensing plates at a location immediately above the fiberglass chevron wicks that collect condensate. The brine gutters are centered over these fiberglass strips. The combined thickness of the gutter plus two layers of nonwoven fiberglass is several mils wider than the gap between condensing plates. When the plate stack is compressed, the gutters are firmly held in place at a location above the fiberglass chevron wicks that collect condensate. After compression by the gutters, the nonwoven fiberglass strips remain sufficiently porous to carry the condensate that forms on the condensing plate past the brine gutter to the chevron condensate wicks.

When assembled the brine wicks sit within the brine gutters. A narrow layer of nonwoven fiberglass sewn to each side of the bottom edges of the brine wicks (i.e., the "edge strips" shown in Figure 25) keep the wicks centered within the gutters. During operation when the condensing plates get hot and expand, the gutter is pulled downward by about ½" relative to the wicks. With sidewalls that are 1" in height, the bottom edges of the wicks remain within the gutters under all operating conditions.

Between October 11 and October 14, the 10-plate Design 11 model operated at hot-brine temperatures between 85°C and 92°C for approximately 15 hours. Measurement of the collected condensates conductivity indicated a significant crossover of fluid from the brine wicks to the condensing plates.

A post-test inspection of the model showed a failure of the narrow layers of nonwoven fiberglass that had been sewn to the bottom edge of the brine wicks. Under the slight abrasion that occurs between these fiberglass pieces and the sidewalls of the brine gutter during thermal cycling, several pieces had broken loose of the brine wicks. In several locations, the detached ends of these pieces had been pushed out of the brine gutters and into contact with the condensing plates.

After removing all the narrow fiberglass layers from the bottom edges of the brine wicks, the Design 11 model was reassembled and operated on October 20. This test was stopped after about three hours when high flow rates of brine were detected in the condensate.

A post-test inspection of the model showed warping of several condensing plates in their hottest section (i.e., upper 15" of the plates). The warping was sufficiently severe to cause contact between the condensing plate and one of its neighboring wicks.

It is most likely that the warping of the condensing plates is caused by differential thermal expansion of different parts of a condensing plate. As shown in the left photograph in Figure 24, titanium cover plates are bonded to the 2-mm Coroplast plate that is the base for each condensing plate. Since titanium has a Coefficient of Thermal Expansion (CTE) that is a factor of 20 times smaller than the CTE for polypropylene stresses will develop within the polypropylene plate during heating when the bonded titanium cover plate limits the expansion of the underlying polypropylene plate. We expect these stresses are causing the polypropylene plate to buckle.

<u>Design 12 – December 2021</u>

Design 12 incorporated the following major changes:

- To prevent bulging of the bottom cover plates, which must support a much higher internal pressure than the top cover plates, the cover plates were converted from thin, 20 mil titanium plate to 4-mm Coroplast. At 4-mm, the thickness of the bottom cover plates now matches the gap between condensing plates. The stack of condensing plates and

bottom cover plates are now kept in compression by the lower U-channel brackets with all forces on the bottom cover plates balanced within the compressed stack.

- The stresses caused by differences in thermal expansion of parts made from different materials was eliminated by replacing the titanium cover plates at the top of the condensing plates with cover plates made from 3-mm Coroplast. The 3-mm Coroplast cover plates extended 1" beyond each edge of the condensing plate. Rectangular pieces of 2-mm Coroplast filled the gaps between pairs of 3-mm Coroplast cover plates in the "overhang" region. The two 1" extensions of each pair of 3-mm Coroplast cover plates rested on the Teflon blocks.
- The switch to top cover plates made from 3-mm Coroplast greatly reduces the size of the gaps between condensing plates that the brine wicks pass through. To ensure no crossover of brine onto the condensing plates in these narrow gaps, each brine wick is contained within a thin polypropylene film sleeve. The upper edge of the bag extends to the upper edge of the wicks and the lower edge extends slightly below the bottom edge of the top cover plate.
- The chevron condensing wicks of Design 11 are eliminated. The flutes in the 4-mm bottom cover plates are adapted to collect the condensate that flows down the condensing plates.
- The means to feed hot brine onto the tops of the wicks is changed so that the two sheets of the wick are separated at the top and the space between the sheets is filled with a strip of cellulose sponge. Metered streams of hot brine were delivered to the sponges.
- The wicks were no longer hung, but each wick instead rested in a single, inclined gutter. The gutters were a custom extrusion fabricated by Seagate plastic with a cross sectional profile that keep the wicks centered in the gutter.
- All plate-to-plate fluid seals were formed from custom molded silicone.

Photographs showing the preceding design features are shown in Figure 26.

Design 12 operated under power from 12:20 pm December 23 to 9:45 am December 24, 2021. The 10-plate model produced clean condensate (68 microS at 3:25 pm) until about 5:30 pm when the conductivity of the condensate increased to over 1 mS. At 7:00 pm the brine flow rate was decreased from about 0.38 gpm to 0.27 gpm. Following this decrease in brine flow, the purity of the condensate improved dramatically: it stayed between 80 and 200 microS from 9:00 pm to at least 1:04 am. Purity slowly degraded to 380 microS at 5:11 am and then rapidly degraded to 5.4 mS at 7:50 am.

The thermal performance of the Design 12 model was poor. At 4:34 am on December 24, with hot brine delivered to the wicks at 87.2^{o}C, the measured temperature-based GOR for the model was 9.7 and the brine conversion fraction was 5.88%. Considering the very low flow rate of brine, both the measured GOR and conversion fraction were low—our EES model of the process predicted a temperature-based GOR of 18.4 and a conversion fraction of 8.59%.

Figure 26 – Design 12 Assembly

A post-test inspection of the Design 12 model uncovered the following problems:

- The yellow sponges that distribute brine across the top of the wicks (as shown in the upper right-most photograph in Figure 26) had broken down under the high operating temperature; the sponges lost their porosity leading to brine overflowing from the polypropylene sleeves that enclosed the top of the wicks.
- As shown in the left photograph of Figure 27, The 3-mm top cover plates, which support the hanging plates (as shown in the upper leftmost photograph in Figure 26) were not sufficiently rigid to keep the top of the condensing plates flat.
- As shown in the right photograph of Figure 27, the U-shaped gutters that collected the brine that flowed off the wicks distorted under the compression that was applied to keep them fixed in place; some opened wider and some closed narrower; One gutter closed to an extent where it pinched the wick leading to loss of brine from the gutter (red circle).

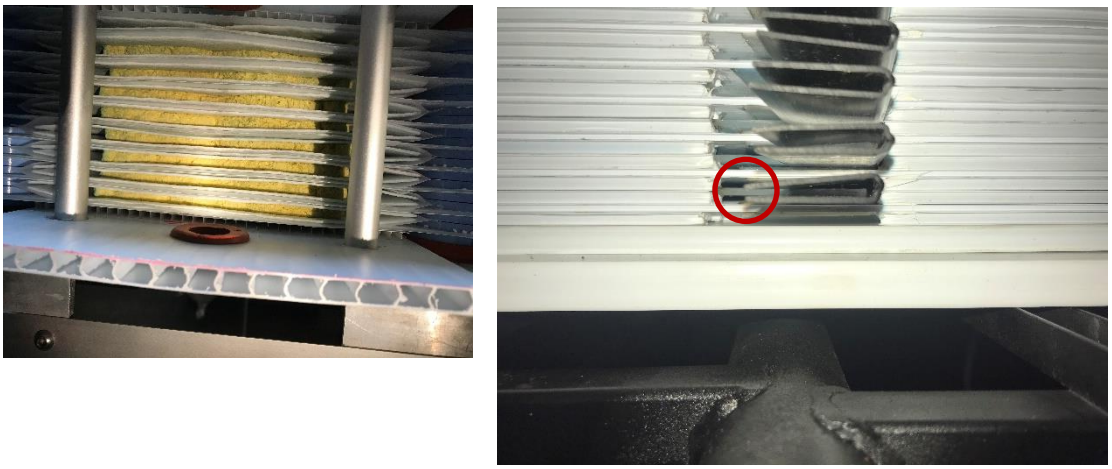

Figure 27 – Post Test Inspection of Design 12

The physical degradation of the Design 12 model that occurred during the test and which caused brine to leak into the condensate is probably not the cause of the model's poor thermal performance. Based on prior operating experience, we suspected that a flow non-uniformity for the brine flowing upward within a condensing plate was the source of the poor thermal performance.

Each condensing plate has on the order of 100 internal flutes. These flutes connect to a common supply pocket at the bottom of the plate and a common collection pocket at the top of the plate. Pressure non-uniformities within the supply pocket can produce flute-to-flute flow variations.

As shown in Figure 28, a flow visualization test in which a slug of blue dye is injected into the line feeding fluid to a plate identified a zone of very low flow in the central flutes of the plate.

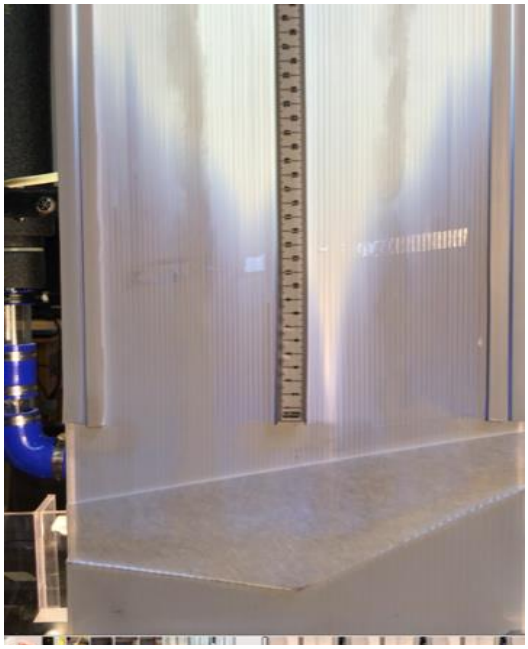

Figure 28 – Flow Non-Uniformity within A Condensing Plate

Figure 29 – 1 GPM Processor Installed at the USBR Yuma Desalting Plant

The zone of low flow is most likely caused by the location of the supply and collection ports for each plate, which are at the corners of the plate. (As described in a following section, future work will address the problems identified in the operation of the Design 12 model.)

Competition for the Solar Desalination Prize

In April 2021, AILR was notified that its BrineZero entry to the competition for the Solar Desalination Prize, which is based on the DGD technology under development in this project, was selected as one of eight semifinalists. In the next round of the competition to select finalists, AILR will prepare a detailed design and implementation plan for a 5-gpm DGD brine concentrator to operate powered by solar thermal collectors. This next round of the competition closes in April 2024.

The More Water, Less Concentration Competition

In July 2021, AILR was notified that their DGD technology was selected as a finalist in the "More Water, Less Concentrate" competition sponsored by the U.S. Bureau of Reclamation. Based on the work in this SBIR award, AILR designed, fabricated and tested the 1-gpm brine concentrator shown in Figure 29 at the USBR Yuma Desalting Plant for one week starting on June 21, 2022. (Although not conducted under the Phase II SBIR award, the USBR Yuma test is part of our commercialization efforts for the DGD technology and in part is documented in this section of the final report.)

The Commercial Potential for a DGD Facility for Processing RO Concentrate

Our entry in the USBR competition was designed to recover at least 90% of the water in a 1 gpm stream of RO concentrate in three modules each composed of 70 plates. Although we were not able to operate at the maximum design temperature of 95^{o}C, monitored operation during the first three days of testing did confirm the performance projections of our design software at peak operating temperatures up to 82^{o}C. With the assumption that work in the future will produce a design that operates reliably at 95^{o}C and meets or exceeds the performance projections of our design software, we have scaled up our 1-gpm design to a full-scale plant that has a water recovery of 95% when processing 100,000 gpd of RO concentrate. Salient features of the full-scale plant that uses the DGD technology are:

- RO concentrate is processed from 8,000 ppm TDS to approximately 200,000 ppm TDS in seven stages.
- The basic element of the processing unit—the condensing plate and wick pair—duplicates that used in the USBR competition. Modifications are made to the plate-to-plate spacing elements used in the competition's modules to stabilize the assembly.
- A "unit" processing module is an insulated stack of approximately 320 plates (which is a modest scale-up of the 70-plate stacks used in the competition).
- As shown in Table 1, the first stage processes the highest volume of brine (69.4 gpm) in 41 modules, increasing brine TDS from 8,000 to 19,300 ppm; the first-stage discharge is the second-stage feed, the second-stage discharge is the third-stage feed, etc.; the final seventh stage concentrates 3.4 gpm of brine from 162,000 ppm up to 193,000 ppm in a single module.
- The seven-stage processor has 70 modules arranged in a 7 x 10 array. With 40-inch aisles between strings of modules, the building for the processor has a footprint of 51' x 92' (4,700 ft2).
- Projected installed cost for the 100,000 gpd brine concentrator is $511,000. This is based on: 1) the material, labor and tooling costs to produce 70 modules is $256,000 (where actual material costs for the 1-gpm pilot for the competition have been discounted by about 25% to allow for high volume purchases), and 2) a 2.0 multiplier has been applied to the cost for the modules to estimate the installed cost for the fully functional installation.

Similar to the operation of our entry in the USBR competition, the full-scale DGD brine concentrator would process concentrate that was received directly from the RO facility (i.e., no pretreatment would be required other than that required by the RO facility.)

The DGD process is designed to operate with the continuous precipitation of reverse soluble salts (e.g., CaSO4) in a hot, seeded precipitation tank that is immediately upstream of the processor's wicks. With hot brine in phase-equilibrium before flowing onto the wicks, reverse-soluble salts stay in solution as the brine flows down the wicks and cools by evaporation.

Table 1 – Seven-Stage Operation of a 100,000 GPD Brine Concentration Facility

Stage		1	2	3	4	5	6	7	Total
Brine Feed Temp	C	30.0	30.0	30.0	30.0	30.0	30.0	30.0	
Brine Preheat Temp	C	91.9	91.7	91.1	90.4	89.6	88.9	88.1	
Brine Max Temp	C	95.0	95.0	95.0	95.0	95.0	95.0	95.0	
Brine Discharge Temp	C	33.4	33.7	34.2	35.0	35.8	36.5	37.3	
Brine/Condensate Delta	C	3.2	3.5	4.0	4.8	5.6	6.3	7.1	
Brine Feed	gpm	69.4	28.7	16.0	8.9	5.7	4.1	3.4	
C Input	ppm	8,000	19,327	34,729	62,289	98,208	135,064	162,235	
C Output	ppm	19,327	34,729	62,289	98,208	135,064	162,235	193,306	
BPE	degC	0.30	0.65	1.30	2.20	3.20	4.00	5.00	
Water Vapor Flux	LMH	0.380	0.369	0.350	0.322	0.292	0.268	0.238	
condensate	gpm	40.7	12.7	7.1	3.3	1.5	0.7	0.6	
Stage GOR		18.94	17.28	14.46	11.14	8.24	6.52	5.12	16.36
Q Thermal	kW-th	314.7	108.0	71.7	42.9	27.4	15.5	15.7	
Brine Recirculation	gpm	414.9	135.3	81.0	41.6	22.3	11.0	10.1	
nAssemblies		41	13	8	4	2	1	1	70
								recovery	95.9%

Although much longer operating times at maximum temperature closer to 95°C are required than were achieved in the USBR competition to prove the effectiveness of the hot, seeded precipitation tanks used by a DGD processor, experience during the competition and the post-test inspection of the wicks tended to support the design goal of preventing salt/scale accumulation on the wicks by collecting reverse-soluble salts in a serviceable, hot, seeded precipitation tank located immediately upstream of the wicks.

The primary energy input to the DGD process is steam at slightly above one-atmosphere pressure. A first-generation processor would use a steam boiler fired by natural gas. The gain output ratio (GOR) for each stage appears in Table 1. With the earlier stages producing most of the product condensate, the average gain output ratio (GOR) for the processor is projected to be 16.4 (i.e., 16.4 pounds of product condensate per pound of input steam). The steam generator for the 100,000 gpd processor must then supply steam at 2,000 lb/h (i.e., 2.5 mmBtu [750 kW] firing rate). An automated, closed-loop controller would modulate the firing rate of the steam generator to maintain the hot-brine feed to the Brine Zero modules at a prescribed setpoint (i.e., 95°C). The steam generator would operate on mineral-free condensate produced by the DGD processor and have minimal O&M requirements.

Assuming that steam is provided to the DGD facility by an 80% efficient boiler fired by natural gas priced at $0.0188 per kWh-thermal (i.e., the average price paid by industrial customers in Arizona in 2021), the cost of water recovered from RO concentration breaks down as follows,

Energy Cost	$0.928 per m3
Capital Cost	$0.357 per m3
O&M Cost	$0.260 per m3
Total Cost	$1.545 per m3

(where Capital Cost has been projected using the preceding $511,000 installed cost for a 100,000 gpd plant that is amortized over 12 years operating at a capacity factor of 0.9; and the O&M costs are a rough estimate that match reported O&M costs for a brackish water RO facility operating without brine concentration[6].)

As reported in Reference 6, the average cost of water supplied by seven brackish water RO plants in Texas in 2011 was $0.487 per cubic meter (in 2021 dollars). Assuming that the initial processing in the RO plant recovers water at 70% efficiency, and the DGD process recovers 95% of the water from the RO concentrate, the blended cost of water from the plant is $0.801 per cubic meter.

Although a 95% water recovery from RO concentrate at a cost of $1.545 per cubic meter is low compared to the cost for conventional brine-concentration means, the impact on the blended cost of water is significant (i.e., 64% increase from $0.487 to $0.801). We do note that the largest component in the COW for the DGD process is for energy. In this analysis, the industrial cost of natural gas was relatively high--$0.0188 per kWh-thermal in 2021 versus $0.0134 per kWh-thermal in 2019 (the last full year not affected by the pandemic). With natural gas at 2019 prices, the blended cost of water would decrease from $0.801 to $0.722 per cubic meter—a cost for water that approaches the $0.60 per cubic meter target that we had previously identified as competitive in the California market for agricultural water.

We also note that the DGD process can be directly driven by steam produced by solar thermal collectors. As previously reported, AILR is now competing for the Solar Desalination Prize. All entries in this second competition must operate on thermal energy provided by solar collectors. AILR's entry will be driven by steam produced within an array of evacuated-tube collectors. In a sunny, Southwest location, AILR's solar collectors are projected to supply thermal energy at less than $0.015 per kWh-thermal. A DGD facility operating in Arizona, driven by AILR's steam-generation collectors and backed-up with natural gas would provide a low-cost means of desalting brackish water that had a very low carbon footprint.

Conclusion and Path to Commercialization

The design of a DGD processor for brine concentration that operates reliable for long periods at high efficiency has proved challenging. Operational problems have been encountered both in the twelve different designs that have been tested during the three years of the Phase II SBIR work

[6] Arroyo and Shirazi, "Cost of Brackish Groundwater Desalination in Texas," www.twdb.texas.gov, September, 2012.

and the USBR competition, and the sources of the problems have been identified. Although experience has shown that solutions to one problem can sometimes create new problems, we believe we are converging on a design that will meet all performance metrics regarding cost, efficiency and reliability. In particular, we are now working towards the demonstration of a 30-plate module with the following features:

- Each condensing plate will have a single, centrally located port at its top where brine is collected from the plate; each plate will have two bottom corner ports delivering brine to the plate; these changes have been proven to create a much more uniform flow of brine within the plates.
- Each wick will have two half-width pockets at their top that receive hot brine from the two distributor pipes—one on each side of the central collection port; with smaller pockets, sponges are no longer needed to spread brine across the wicks' upper edges; with the sponges eliminated, much higher per-plate flows of brine can be processed without overflowing the sleeved pockets at the top of the wicks.
- Brine gutters with a profile that keeps the wicks centered within the gutter will replace the U-channel gutters used in Design 12; the new profile will also prevent the gutters from cocking in the gap between condensing plates.
- The basic element of the processing unit—the condensing plate and wick pair—will duplicate that used in the USBR competition, but with modifications made to the plate-to-plate spacing elements to stabilize the assembly.

Further development towards commercialization of the DGD processor is now most likely to occur as part of the Solar Desalination competition. Following the successful operation of the 30-plate module previously described, we will submit a proposal for field operation at a farm in Ventura California under the Solar Desalination competition.

California's agricultural industry, with total exports in 2020 of $21 B, desperately needs new water resources, as do farmers throughout the Southwest. Brackish water aquifers are a promising new resource but the cost to upgrade brackish water to irrigation quality is now too high to meet the needs of all but the highest value crops. Although the DGD technology is not ready for commercial introduction, the work performed under the Phase II SBIR award, the USBR competition and the Solar Desalination competition has shown a path to commercialization that has the potential to meet the very tight economic constraints imposed by the agricultural industry.